AFRL-RX-WP-TP-2011-4404

MODEL BASED STUDIES OF THE SPLIT D DIFFERENTIAL EDDY CURRENT PROBE (PREPRINT)

Jeremy Knopp and Mark Blodgett

Metals, Ceramics & Nondestructive Evaluation Division (AFRL/RXLP)

R.D. Mooers

University of Dayton Research Institute

NOVEMBER 2011

Approved for public release; distribution unlimited.

See additional restrictions described on inside pages

STINFO COPY

AIR FORCE RESEARCH LABORATORY
MATERIALS AND MANUFACTURING DIRECTORATE
WRIGHT-PATTERSON AIR FORCE BASE, OH 45433-7750
AIR FORCE MATERIEL COMMAND
UNITED STATES AIR FORCE

REPORT DOCUMENTATION PAGE

Form Approved
OMB No. 0704-0188

1. REPORT DATE *(DD-MM-YY)*
November 2011

2. REPORT TYPE
Technical Paper

3. DATES COVERED *(From - To)*
1 September 2011 – 1 September 2011

4. TITLE AND SUBTITLE
MODEL BASED STUDIES OF THE SPLIT D DIFFERENTIAL EDDY CURRENT PROBE (PREPRINT)

5a. CONTRACT NUMBER
In-house

5b. GRANT NUMBER

5c. PROGRAM ELEMENT NUMBER
62102F

5d. PROJECT NUMBER
4349

5e. TASK NUMBER
40

5f. WORK UNIT NUMBER
LP111200

6. AUTHOR(S)
Jeremy Knopp and Mark Blodgett (AFRL/RXLP)
R.D. Mooers (University of Dayton Research Institute)

7. PERFORMING ORGANIZATION NAME(S) AND ADDRESS(ES)
Nondestructive Evaluation Branch/Metals, Ceramics & Nondestructive Evaluation Division
Air Force Research Laboratory, Materials and Manufacturing Directorate
Wright-Patterson Air Force Base, OH 45433-7750
Air Force Materiel Command, United States Air Force

University of Dayton Research Institute

8. PERFORMING ORGANIZATION REPORT NUMBER
AFRL-RX-WP-TP-2011-4404

9. SPONSORING/MONITORING AGENCY NAME(S) AND ADDRESS(ES)
Air Force Research Laboratory
Materials and Manufacturing Directorate
Wright-Patterson Air Force Base, OH 45433-7750
Air Force Materiel Command
United States Air Force

10. SPONSORING/MONITORING AGENCY ACRONYM(S)
AFRL/RXLP

11. SPONSORING/MONITORING AGENCY REPORT NUMBER(S)
AFRL-RX-WP-TP-2011-4404

12. DISTRIBUTION/AVAILABILITY STATEMENT
Approved for public release; distribution unlimited.

13. SUPPLEMENTARY NOTES
The U.S. Government is joint author of this work and has the right to use, modify, reproduce, release, perform, display, or disclose the work. PA Case Number and clearance date: 88ABW-2011-4921, 14 Sep 2011. Preprint journal article to be submitted to Review of Progress in QNDE. This document contains color.

14. ABSTRACT
This paper presents preliminary modeling work of split D differential probes, in both regular differential and reflection modes. This work is a prelude for a more in-depth model validation study using split D type probes. A modeling comparison is made for both air and ferrite cores. Lastly, numerical and experimental results are compared.

15. SUBJECT TERMS
Split D, differential, reflection differential, eddy current, VIC 3D©, ECSIM

16. SECURITY CLASSIFICATION OF: a. REPORT	b. ABSTRACT	c. THIS PAGE	17. LIMITATION OF ABSTRACT:	NUMBER OF PAGES	19a. NAME OF RESPONSIBLE PERSON (Monitor) / 19b. TELEPHONE NUMBER (Include Area Code)
Unclassified	Unclassified	Unclassified	SAR	10	Mark Blodgett / N/A

MODEL BASED STUDIES OF THE SPLIT D DIFFERENTIAL EDDY CURRENT PROBE

R. D. Mooers[1], J. S. Knopp[2], M. P. Blodgett[2]

[1]University of Dayton Research Institute, Structural Integrity Division 300 College Park Drive, Dayton, OH, 45469
[2]Air Force Research Lab, NDE Branch, Wright Patterson AFB, OH, 45433

ABSTRACT. This paper presents preliminary modeling work of split D differential probes, in both regular differential and reflection modes. This work is a prelude for a more in-depth model validation study using split D type probes. A modeling comparison is made for both air and ferrite cores. Lastly, numerical and experimental results are compared.

Keywords: Split D, Differential, Reflection Differential, Eddy Current, VIC 3D©, ECSIM,
PACS: 81.70.Ex, 02.70.-c

INTRODUCTION

Differential eddy current probes are used for the detection of surface breaking defects in bolt/ bore holes, around fastener sites, and in tubing and pipelines. Differential probes are sensitive to flaws like other eddy current probes, but any possible enhancement of this sensitivity is dependent on the nature of the problem or inspection. Differential probes are invariant to subtle changes in geometry, material properties, temperature, probe wobble (slight changes to vertical orientation), and lift off. This invariance is due to the differential signal produced by the use of two (2) receiver coils [1]. Essentially, the receive coil responses are subtracted from one another. When this subtraction occurs over a defect free region, there is no net response. Differential probes exhibit noise reduction properties when used in an inspection and are known to have a higher signal to noise ratio. The focus of this work is to provide an assessment of state-of-the-art eddy current modeling. Models are created for various differential and reflection differential split D style probes with both air and ferrite cores. This initial work is in progress and more model validation and benchmarking studies are in progress.

BACKGROUND RESEARCH

Differential coils have been investigated quite extensively, both experimentally and through modeling, due to the numerous advantages they have in many common inspection situations. Much of this research has focused on differential coils that are composed entirely of circular coils. Depending on the orientation, probes composed of circular coils can be configured to operate in both differential and reflection differential mode. The most common form is the bobbin coil, shown in Fig. 1a, which is used in tubing and pipe inspection. Numerous experimental and modeling research efforts have investigated this type of probe [2-5]. The probes employed in [6, 7] are examples of reflection differential probe composed of circular coils. These probes are composed of three circular coils; two operate as a differential receiving pair with the final coil operating as a drive coil. They can be designed with the drive coil either surrounding or leading the receiving pair. Basic top view diagrams of these probes are shown in Fig. 1b and 1c. The image shown in Fig 1b is based off the design from TEAM (Testing Electromagnetic Analysis Methods) Problem 8. One configuration that has not been extensively addressed in the research is the Split D type. These probes operate in the same manner as other differential and reflection differential probes, but the shape of the drive/receive coils have been altered. This probe design allows for more efficient use of space, and a smaller footprint in certain circumstances. Figure 1d below shows a top view diagram of a shielded reflection differential probe. There have been efforts to model these types of probes, and some of this has been implemented into modeling software packages [8, 9]. Some experimental studies of these probes have been reported [9].

GENERIC PROBE MODELING

Generic Model Parameters

Differential and reflection differential models were first created for a generic probe, with dimensions that approximate an actual probe. The majority of the input parameters were estimated or interpolated from a few approximate values obtained through a probe manufacturer. The estimated and interpolated values can be found in Table 1. Both probe configurations were modeled with air and ferrite cores.

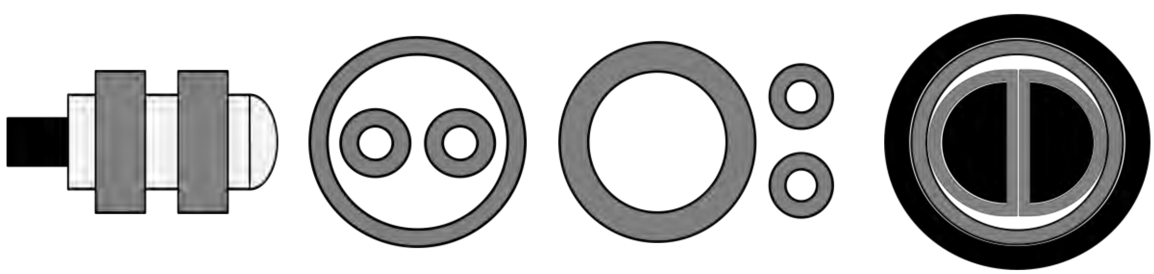

(a) (b) (c) (d)

FIGURE 1. Collection of various differential and reflection differential probe designs: (a) Bobbin Probe, (b) TEAM Workshop Problem 8, (c) Reflection Differential Sliding probe, (d) Split D Design

TABLE 1. Dimensions for generic probe modeling exercise

D Core Dia.	2.00 mm	D Coil Thickness	0.0735 mm
D Core Height	4.00 mm	D Coil Windings	150
Core Gap	0.15 mm	Drive Coil Inner Diameter	2.20 mm
Core Relative Permeability	200	Drive Coil Outer Diameter	2.70 mm
D Coil Dia.	2.00 mm	Drive Coil Height	2.50 mm
D Coil Height	2.50 mm	Drive Coil Windings	120

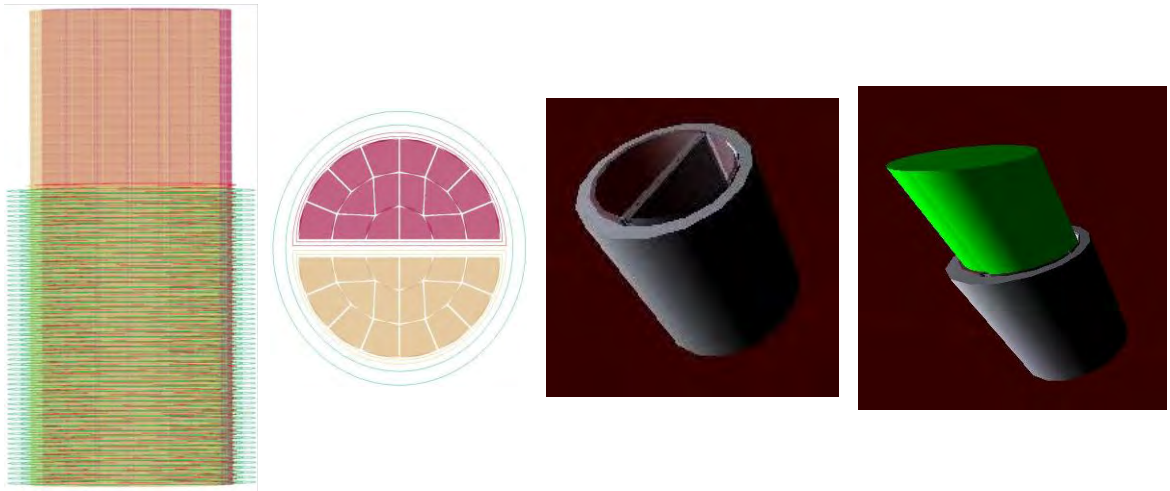

(a) (b) (c) (d)

FIGURE 2. Generic Split D Reflection Differential Probes Models: (a,b) ECSIM, (c,d) VIC 3D©

The images seen in Fig. 2 are representative of the reflection differential models created. The circular drive coil in VIC 3D© was modeled as a racetrack coil with a straightaway length of zero (0) to ensure a correct mesh of the various probe components. To ensure the correct reproduction of the differential signal, the scale factor, VIC 3D©, and the coil polarity, ECSIM, were adjusted. The scale factor and coil polarity alter the assumed direction of current flow in the receive coils. Due to the rotation needed to model the D coils in VIC 3D© each coil employed the same value. In ECSIM, the coil values must be opposite to give the proper signal. The differential probe models had values of (1,1) and (1,-1) while the reflection differential models employed values of (1,0), (0,1), and (0,-1) for the drive and D coils respectively.

The modeled test specimen was a semi-infinite block 5 mm thick with conductivity of 1.02 MS/m. The modeled defect was a rectangular notch placed in the center of the test specimen with dimensions of 2 mm x 1 mm x 0.5 mm for length, depth, and width respectively. A test frequency of 200 kHz was used. The probe was oriented such that the flat portion of the D coils were perpendicular to the notch length. Simulated scans were 10 mm in length centered over the notch with 0.1 mm spacing.

Results and Discussion

With the exception of the air-cored reflection differential models, results will be presented for all modeled configurations. Figure 3 shows the results for the air-cored differential models. Closer inspection of the amplitudes of the data sets in Fig. 3 reveals that there is moderate agreement in the reactance component and very good agreement in the resistance component. The overall percent difference or amplitude variation is 27% for the reactance and 2.2% for the resistance. The transition region between the main peaks is an area of large discrepancy in the curve shape. VIC 3D© shows a smooth transition in the resistance component and a sharp transition in the reactance. ECSIM shows a set of smaller secondary peaks in both components. There are also slope discrepancies between the two data sets in the region around $x = \pm 3$. These slope discrepancies could be the results of differences in the how the D cores and coils are modeled.

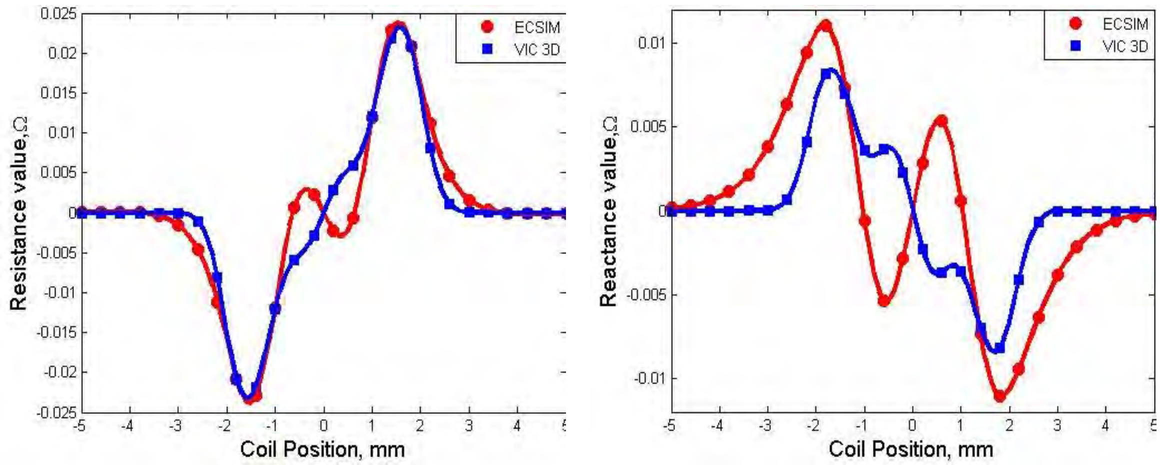

(a) (b)

FIGURE 3. Results for generic Air Cored Split D Differential, (a) ΔR, (b) ΔX

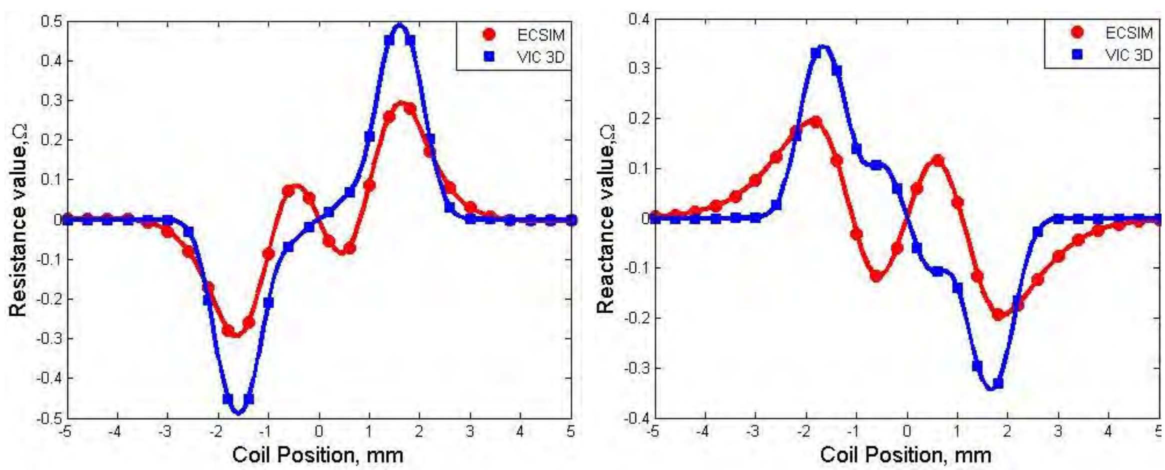

(a) (b)

FIGURE 4. Results for generic Ferrite Cored Split D Differential, (a) ΔR, (b) ΔX

Figure 4 shows the results for the ferrite cored differential probe. The amplitude variation is significantly more than the air-cored models. The average overall amplitude variation has increased from 14.5% in the air-cored models to 52% in the ferrite-cored models. The secondary peaks in the ECSIM data sets have also increased in amplitude relative to the main peaks. The variations in the transition zone and the slopes appear again. There is little change in the curve shape between air and ferrite cored models, but the overall amplitude is an order of magnitude greater than the air-cored case.

The amplitude variation for the ferrite cored reflection differential models, Fig 5, is over double that seen in the ferrite cored differential models. The shape variations seen in the ferrite cored differential simulations have been reduced. The transition regions of both data sets show smaller secondary peaks; however, the discrepancy in the slope still exists. In addition, the locations of the major peaks in the individual data sets are shifted relative to one another. The changes in curve shape become more apparent if the data sets are normalized to a maximum value of one (1). In addition, upon normalizing the data it becomes more evident that the secondary peaks have the same amplitude relative to the main peaks in each data set.

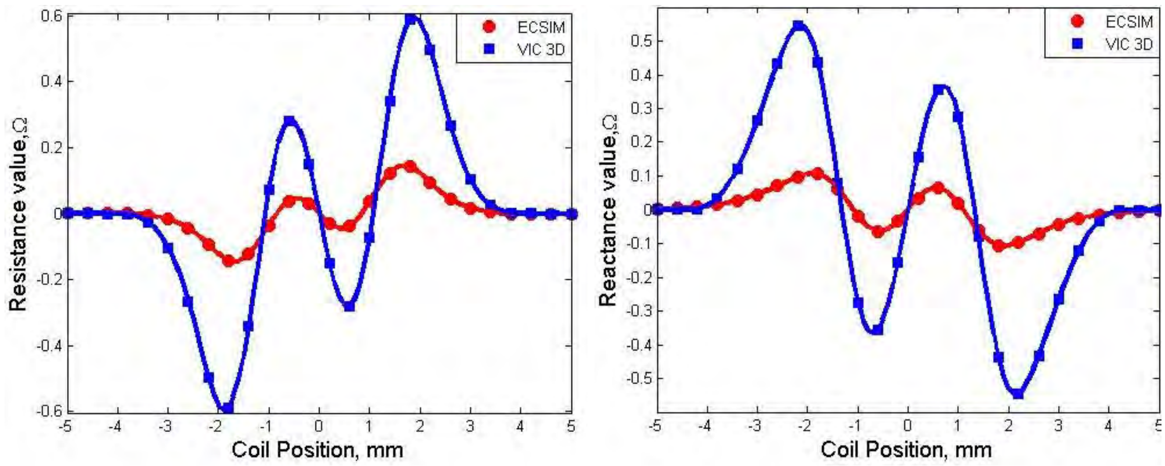

(a) (b)

FIGURE 5. Results for generic Ferrite Cored Split D Reflection Differential, (a) ΔR, (b) ΔX

EXPERIMENTAL PROBE MODELING

<u>Experimental Setup</u>

As a second exercise the simulations codes were compared to experimental data taken using a commercial differential pencil probe. Data was acquired with a Nortec $19e^{II}$ in conjunction with a three-axis scanning stage. To maximize the on screen signal at the two test frequencies, 500 kHz and 2 MHz, the horizontal and vertical gains were set to 80 dB. The phase angle was set to zero to allow comparison between the individual components and the simulation data.

The test specimen was a Ti-6Al-4V plate roughly 6.35 mm thick with a series of EDM notch equally spaced down the center. These notches range in nominal length from 0.508 to 2.54 mm and have an aspect ratio of 2:1. The EDM notch chosen for this test has dimensions of 2.5 mm x 1.3 mm x 0.127 mm for length, depth, and width respectively. The probe was aligned by manually scanning in both directions over the notch and looking for a midpoint in the observed data curve. The system was nulled away from the notch to get the desired response. Data was collected at positions over the length of the notch ranging ± 6.2 mm in length from the center of the notch with spacing of 0.1mm.

Figure 6 shows images of the probe used for the experimental measurements. The needed model input parameters were determined from the close up image in Fig. 6b. By using a known probe dimension and Fig. 6b the majority of the dimensions found in Table 2 could be interpolated. The few remaining dimensions were estimated.

TABLE 2. List of probe dimensions for experimental comparison

D Core Dia.	1.40 mm	D Coil Thickness	0.1 mm
D Core Height	1.23 mm	D Coil Windings	150
Core Gap	0.20 mm	Shielding Inner Diameter	1.80 mm
Core Relative Permeability	200	Shielding Outer Diameter	2.45 mm
D Coil Dia.	1.40 mm	Shielding Height	2.25 mm
D Coil Height	0.60 mm	Shielding Relative Permeability	200

(a)

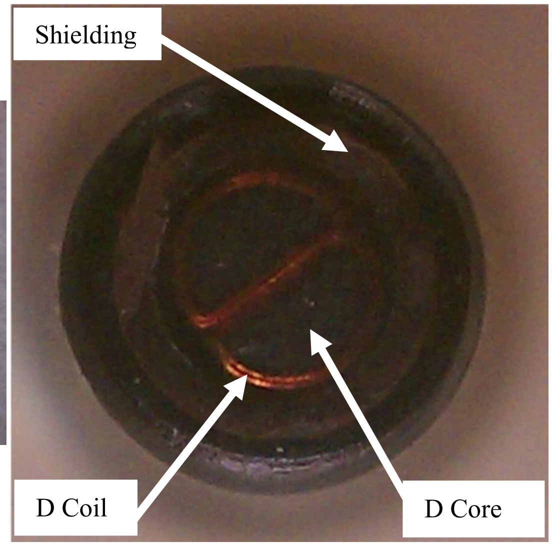

(b)

FIGURE 6. Experimental split D differential probe, (a) full probe, (b) close up of probe face with coil and cores and shielding labeled

Experimental Probe Modeling

The shielding adds another level of complexity to the model. For the ECSIM probe models, everything is modeled as in the previous ferrite cored differential models with the addition of an appropriately meshed hollow circular cylinder included for the shielding. In VIC 3D© the different portions of the probe must be modeled in a certain order to obtain an accurate and working probe model. A solid circular cylinder with the desired shielding outer diameter is modeled first. A zero permeability solid cylinder with an outer diameter equal to the desired shielding inner diameter is centered inside this to create a hollow circular cylinder with appropriate shielding dimensions. The coils and cores can then be modeled as before to create the entire probe. The core properties and D coil windings were held constant from the previous ferrite cored differential models. The relative permeability of the core and shielding were set equal for model simplicity.

Results and Discussion

The Nortec is only able to provide a relative measure of the change in amplitude and phase. Consequently, an absolute amplitude comparison between the experimental and the simulation data is not possible. However, by normalizing each set of data to a maximum positive value of one (1), a comparison of the shape can be made. The images in Fig. 7 show normalized data for all three data sets separated by component, horizontal with resistance and vertical with reactance.

The data in Fig. 7 illustrates the good shape match between the simulation codes and the experimental data. Each code is able to accurately calculate the small perturbations in the resistance component at roughly $x = \pm 2$. The transition region also shows better agreement with smoother transitions in all data sets. In certain simulations, the main peaks are translated with respect to the experimental data. This could be the result of modeling differences or variations in the experimental data. In addition, the experimental data is asymmetric in amplitude. This could be due to variations between the coils, or result from slight misalignment in the experimental scans.

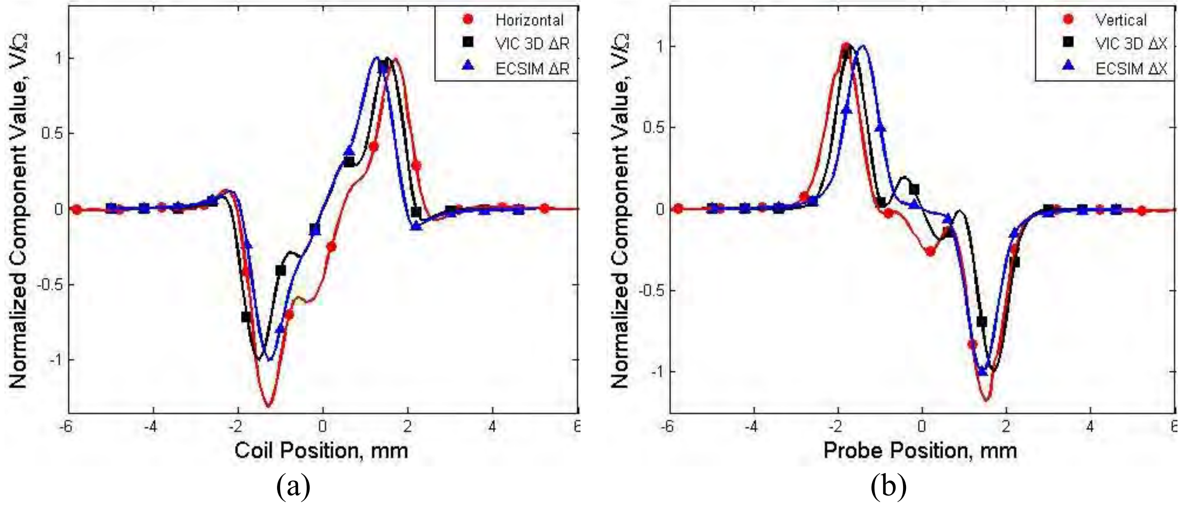

FIGURE 7. Comparison of normalized data plots of simulated and experimental data at 2 MHz, (a) Horizontal and ΔR, (b) Vertical and ΔX

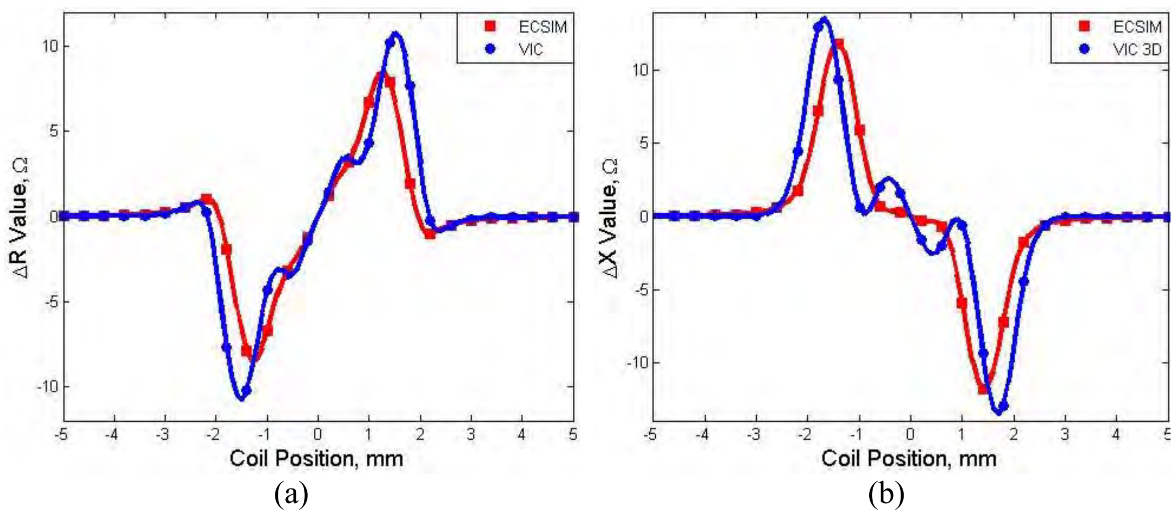

FIGURE 8. Comparison of simulated data at 2 MHz for the experimental probe models, (a) ΔR, (b) ΔX

Figure 8 shows the change in resistance and reactance at 2 MHz for each simulation code. The amplitude discrepancy has been reduced from roughly 50% for both components to 25% and 14% for the resistance and reactance components respectively compared to previous ferrite cored differential models. The transition and slope curve shape discrepancies still appear but are less dramatic. ECSIM shows a smooth transition between the main peaks in both components while VIC 3D© shows the secondary peaks and sharp transition, which is different from the previous models. The main peaks are shifted relative to one another, which could be the result of modeling differences.

SUMMARY AND CONCLUSIONS

This paper presents a model-based study of Split D differential and reflection differential eddy current probes with both air and ferrite cores. Generic models were created in both VIC 3D and ECSIM and the computed resistance and reactance values were compared. The best results were seen in the air cored differential models while the ferrite cored reflection differential models produced the poorest results. A second series of models were created with dimensions interpolated from a commercial differential pencil probe. These models simulate the scanning of the experimental probe over an EDM notch in a Ti-6Al-4V plate. Very good agreement was observed in the normalized shape of the simulation and experimental data sets. The computed resistance and reactance values for these second models also show good agreement.

Continued refinement of the models is necessary to improve the comparison between the models and the experiments for later validation and benchmarking exercises. The need for consistent dimensions has been a critical factor in these tests. There has also been a concern that the two codes differ in the modeling of the D shaped cores and coils. To obtain the most accurate simulations, actual dimensions and properties for the cores and coils must be known and the various components must be modeled in a consistent manner. Certain artifacts seen in the various data sets also need to be investigated to determine the cause, such as the discrepancies in the transition regions.

ACKNOWLEDGEMENTS

The authors want to thank Hal and Elias Sabbagh, Norio Nakagawa, and John Aldrin for their modeling expertise during this project.

REFERENCES

1. B.A Auld, et al. *Research in Nondestructive Evaluation* **Vol. 1 Issue 1**, 1-11 (1989).
2. N.Ida, H. Hoshikawa, and W. Lord, *NDT International* **Vol. 18 Issue 6**, 331-338 (1985).
3. N. Ida, R Palanisamy, W. Lord, *Materials Evaluation* **Vol. 41 Issue 12**, 1384-1394 (1983).
4. D. Premel, G. Pichenot, T. Sollier, *International Journal of Applied Electromagnetics and Mechanics* **Vol. 19 Issue 1-4**, 521-525 (2004).
5. Young Bae Kong, Sung-Jin Song, et al, “Parametric Study for Optimization of Bobbin Coil ECT Probe Design by Electromagnetic numerical Analysis,” in *Review of Progress in QNDE 26A*, edited by D.O Thompson and D. E Chimenti, AIP Conference Proceedings vol. 894, American Institute of Physics, Melville, NY, 2007, 378-385.
6. P. Chaussecourte, *COMPEL-The International Journal for Computation and Mathematics in Electrical and Electronic Engineering* **Vol. 11 Issue 3**, 331-333 (1992).
7. A. Schumm and N. Nakagawa, “Code Validation for Eddy Current Modeling: Tubing Inspection with Reflection Differential Probes,” in *Review of Progress in QNDE 24A*, edited by D.O Thompson and D. E Chimenti, AIP Conference Proceedings vol. 760, American Institute of Physics, Melville, NY, 2005, 509-515.
8. H.A Sabbagh, E.H Sabbagh, and R.K Murphy, “Recent Advances in Modeling Eddy-Current Probes,” in *Review of Progress in QNDE 21A*, edited by D.O Thompson and D. E Chimenti, AIP Conference Proceedings vol. 615, American Institute of Physics, Melville, NY, 2007, 423-429.
9. N. Nakagawa, T.A. Khan, and J. Gray, “Eddy Current Probe Characterization for Model Input and Validation,” in *Review of Progress in QNDE 21A*, edited by D.O Thompson and D. E Chimenti, AIP Conference Proceedings vol. 509, American Institute of Physics, Melville, NY, 2000, 473-480.